

# Porous Carrageenan-Derived Carbons for Removal of Pb(II) Ions from Aqueous Solution

*S M Anisuzzaman*

*Rachel Fran Mansa \**

*Richmond Pillai Elkes*

*Energy and Materials Research Group, Chemical Engineering Programme, Faculty of Engineering, Universiti Malaysia Sabah, 88400 Kota Kinabalu, Sabah, Malaysia.*

\*e-mail: rfmansa@ums.edu.my\_or\_rmansa@gmail.com

*Submitted* 8 February 2023

*Revised* 18 July 2023

*Accepted* 14 August 2023

**Abstract.** Activated carbon (AC) is a widely used adsorbent that can be applied to remove lead (Pb(II)) ions from wastewater. In the current work, carrageenan was used as a precursor to prepare carrageenan based activated carbon (CAC) using potassium hydroxide (KOH) as a chemical activating agent for Pb(II) ions adsorption from aqueous solution of lead nitrate ( $\text{Pb}(\text{NO}_3)_2$ ). The preparation process involved activation of the carrageenan with KOH at a ratio of 1:4 followed by carbonization at  $700^\circ\text{C}$  for 4 h. Physical and chemical characterization of synthesized CAC was conducted to understand surface morphology and functional groups. As the scanning electron microscope (SEM) analysis found, the CAC particle sizes are, on average  $25.11\ \mu\text{m}$  before adsorption and  $39.21\ \mu\text{m}$  after adsorption. Functional group studies proved that the adsorbate had been adsorbed into the CAC by showing a band stretch of the nitrile group in the Fourier transform infrared (FTIR) spectroscopy analysis. The adsorption process was optimized by changing the temperature of adsorption, dosage of adsorbent, and initial concentration of adsorbate. At the optimum conditions, maximum Pb(II) ions adsorption on the CAC was achieved by 99.04%. Throughout this study, the highest capacity of CAC was determined to be  $1.95\ \text{mg/g}$ , while the minimum capacity was found to be  $0.19\ \text{mg/g}$ . Langmuir and Freundlich isotherm were studied to understand adsorption mechanisms. The results suggested that the Langmuir isotherm model fits better than the Freundlich model with a regression coefficient  $R^2$  of 0.9845. Pseudo-first-order and pseudo-second-order kinetic models were applied to test the experimental data. Pseudo-second-order exhibited the best fit data for kinetic studies with a regression coefficient of  $R^2$  0.9996, indicating that the adsorption of lead using CAC is limited by the chemisorption process.

**Keywords:** Carrageenan, Pb(II) ions, Chemical activation, Heavy metal, Isotherm, Kinetics

## INTRODUCTION

The heavy metals are found in wastewater from various manufacturing factories, including material production (leather), glass production, dyes and pigments, metal glazing, and battery

production (Islam et al., 2021). Several hazardous elements were found in wastewater treatment. Arsenic (As), chromium (Cr), lead (Pb), mercury (Hg), copper (Cu), zinc (Zn), cadmium (Cd), nickel (Ni), and manganese (Mn) are among the metals (Yahya et al., 2020). These metals are

toxic pollutants that are not biodegradable, endanger community health, and have economic consequences when discharged into any water source (Roy et al., 2022; Kwak et al., 2019). The constant and unregulated disposal of these pollutants in the atmosphere from various emission sources significantly contributes to one's buildup in freshwater ecosystems, possibly causing long-term damage (Jahan et al., 2022; Hassim et al., 2022). Regrettably, sewage treatment plants are unwilling to eliminate most such substances (Nogueira et al., 2018).

Pb is among the most found heavy metals in wastewater, and it is a powerful oxidizing agent that can be absorbed through the skin (Jaishankar et al., 2014). Nevertheless, most lead levels observed in the environment are indeed the consequence of human activity (Agasti, 2021). Excessive Pb exposure is undoubtedly a major environmental and medical concern affecting children. The harmful effects of Pb on the aquaculture world and the potential danger of contaminating water systems for human consumption inspire programs to curb lead concentrations in municipal pollutant wastewater (Lee et al., 2019). Numerous researchers have sought to eliminate such inorganic and organic contaminants from polluted water bodies using several techniques, including co-precipitation, ion exchange, photocatalysis, electro-coagulation, electroflotation, membrane processes, reverse osmosis, advanced oxidation, adsorption, and so on (Wang et al., 2020; Kavand et al., 2020). These techniques are challenging to achieve due to high operating and maintenance costs, rising energy demands, and non-biodegradability, restricting their potential application. Most systems have limitations such as high initial investment, operational costs, time

utilization, equipment complexity, and removing leftover metallic sludge. As a result, researchers are developing cost-effective and environmentally friendly methods for waste reduction and wastewater optimization. As it's less costly and much more efficient than other techniques, adsorption is the most powerful solution for stripping metal ions away from water sources. Furthermore, the adsorption technique is simple, inexpensive, and environmentally friendly since it may function for an extended time without failure. It requires minimal maintenance, making it a viable option for many. Despite having a high contact area, a micro-porous character, and an adsorption ability, commercial activated carbon (AC). It has relatively high costs (Islam et al., 2021; Wang et al., 2020).

Consequently, an increasingly considerable low-cost product, effective, sourced adsorbents locally for Pb(II) ions adsorption, such as AC derived from sustainable biomasses. AC is produced from biomass raw materials such as coconut shells, sawdust, sugar cane bagasse, fruit stones, apricot stone, pyrolyzed coffee residues, pine bark, pecan shell, peanut shells, palm shell, nutshells (almond, walnut, pecan), almond shells, olive stones, and peach stones is in a growing market (Neme et al., 2022; Khan et al., 2020; Kamal et al., 2019; Alslaiibi et al., 2013). Organic components are abundant in structural heteroatoms (for example, chitosan), which have gone unnoticed but are very captivating due to their ability to yield hetero-doped carbon structures with advanced functionality for plenty of usage (Khan et al., 2020). Recently, carrageenan has attracted attention for sorption applications, where it is widely used to remove pesticides and pharmaceutical contaminants from water due to its natural abundance and good chemical functionality (Laksono et al., 2022;

Kamal et al., 2019; Lapwanit et al., 2018; Nogueira et al., 2018; Mahdavinia et al., 2015). Mesoporous carbon microspheres made from carrageenan, for example, exhibit superior electrochemical capacitance performance due to their large surface area, pore size distribution, and tailored micro- and mesoporous morphology (Keshk et al., 2023; Lapwanit et al., 2018; Nogueira 2018). As a result, it demonstrates that carrageenan is an effective and economical way to create AC compared to other adsorbents. The second issue would be restrictions in establishing adsorbent effectiveness, which is influenced by operational factors like temperature, adsorbent dosage, and time contact. Because of its natural excess and chemical capabilities, carrageenan has attracted attention in adsorption applications, particularly in removing pesticides and toxic pharmacological elements from water (Nogueira et al., 2018). However, carrageenan has received little attention as a carbon source for preparing porous carbon materials.

The two primary methods to produce AC are mechanical and chemical activation. When the two techniques are compared, chemical activation has two significant advantages. Chemical activation, for example, will take place at a lower temperature. Secondly, because there is no need for burn-off char, the percent yield of the chemical activation is significantly greater. Carbonization will occur in the presence of a dehydrating agent such as zinc chloride ( $ZnCl_2$ ), phosphoric acid ( $H_3PO_4$ ), sulfuric acid ( $H_2SO_4$ ), and so on (Song et al., 2010). These additives may lead to cross-links, resulting in a rigorous matrix's generation.

Hence, by conducting adsorption experiments, this study aims to determine the best adsorption model process and the adsorbent's performance towards the

adsorbate. This work used quantitative and instrumental analyses to evaluate the physical properties of CAC to investigate the adsorption process for Pb(II) ions removal from aqueous solutions utilizing carrageenan-based AC (CAC). It was decided to compare different adsorption isotherms and kinetics. The methods for analyzing the effectiveness of adsorption under various operating conditions were also covered, along with the construction of suitable adsorbent isotherm and kinetics models. The physical characterization of CAC, such as bulk density, moisture content, and determination of pH value, were also considered and included in this study.

## MATERIALS AND METHODS

### Materials

In this study, carrageenan was purchased from the local supplier, EvaChem, Malaysia. The carrageenan was in powdered form, white in color, nontoxic, non-fully soluble in water, and slightly pungent smell. For the activation process, the KOH pellet (ChemAR) was supplied by Classic Chemicals Sdn. Bhd. Malaysia. HCl with 37% concentration was purchased from Merck Sd. Bhd. Malaysia. The pure sample of ethanol (solvent) used in this work was obtained from Merck. All chemicals were used without further purification.  $Pb(NO_3)_2$  was obtained from Sigma Aldrich for the adsorption studies.

### Preparation of CAC

One gram of carrageenan was added into 20 mL of water and stirred until the powder fully dissolved, then deposited into a Teflon-lined stainless still autoclave and heated to 200°C for 20 h. The resultant hydro char, a black precipitate was centrifuged (15 min,

6000 rpm, Hettich Zentrifugen, EBA 20), rinsed numerous times with ethanol and water, and dried. In this procedure, KOH was mixed with the carrageenan sample in a 250 mL beaker in a 1:4 ratio (Nogueira et al., 2018). The mixture was then sealed with aluminum foil and thoroughly shaken to ensure KOH could penetrate the sample's interior. A few holes were drilled to allow the vapors to evaporate at room temperature for 24 h. The sample was then dried in the oven at 103°C for 24 h to remove excess moisture from the mixture. 103°C was chosen for the drying process to maximize the removal of any water. These substances were chemically activated using KOH and placed in a tube furnace under a nitrogen environment at 700°C for 4 h. The recovered materials were rinsed using 2 M HCl, followed by distilled water to remove any contaminated chemicals, and then precipitated in ethanol and dried overnight at 60°C.

### Preparation of Adsorbate

A 1000 ppm Pb(NO<sub>3</sub>)<sub>2</sub> solution with 99% purity is dissolved in 1000 mL of distilled water and stirred with a magnetic stirrer to produce a homogeneous mixture. This intermediate solution made three calibration standard solutions with concentrations ranging from 5 to 20 ppm. The calibration curve was created by plotting the absorbance vs. concentration of standard (Pb(NO<sub>3</sub>)<sub>2</sub>) solutions at the characteristic wavelength of 283.3 nm. All samples were prepared in Erlenmeyer volumetric flasks of 100 mL. Nonetheless, for each sample, a calibration graph curve was created. The concentration of Pb(II) ions before adsorption was measured using an atomic adsorption spectrometer (AAS).

### CAC Characterization

The yield of AC is commonly defined as the final weight of AC produced after activation, washing, and drying divided by the initial weight of feedstock, both on a dry basis, as expressed in the Eq. (1):

$$\text{Percentage of yield (\%)} = \frac{\text{Final mass of CAC (g)}}{\text{Initial mass of carrageenan sample (g)}} \times 100 \quad (1)$$

The weighing balance was first zeroed with a beaker of 50 mL volume to calculate bulk density. The beaker was then filled to the 50 mL mark with CAC powder, which was then tapped to ensure no empty spaces formed. The weight was then noted and recorded. The bulk density was then calculated using Eq. (2):

$$\text{Bulk density} \left( \frac{\text{g}}{\text{ml}} \right) = \frac{\text{Mass of CAC (g)}}{\text{Volume of CAC (mL)}} \quad (2)$$

The thermal drying method was used to find moisture content where 1 g of the sample was weighed, put inside the crucibles, and reweighed. The sample was placed in a 105°C oven for 2 to 3 h to maintain a specified weight. The difference between carbon's initial and final mass represents the moisture content. This process was repeated until a constant weight was obtained. The moisture content (%) was calculated using Eq. (3):

$$\text{Moisture content (\%)} = \frac{\text{Initial weight} - \text{Final weight (g)}}{\text{Initial weight (g)}} \times 100 \quad (3)$$

One gram of CAC sample was boiled for 5 min in a glass beaker with 100 mL of distilled water to determine the pH. The solution was diluted to 200 mL and constant stirring after cooling to room temperature.

---

The pH was provided with a detailed pH meter (Eutech Instruments Ecoscan pH meter).

Fourier transform infrared (FTIR) spectroscopy analysis was used to identify the functional groups on the surface of CAC. This analysis could detect the removal of  $\text{Pb}(\text{NO}_3)_2$  solution by CAC before and after adsorption because the adsorbate can bind to the CAC adsorption sites. High spectral resolution data was collected in  $400\text{ cm}^{-1}$  and  $4000\text{ cm}^{-1}$  using Bruker Model Spectrum 100.

Scanning electron microscope (SEM) (Hitachi) instrument visualizes the CAC's microstructure and surface morphology. Furthermore, the orientation of the CAC was assessed using SEM, which affects its mechanical properties. The entire procedure was carried out inside a vacuum chamber. The porous structure of the CAC sample was seen using a SEM. The magnification was adjusted to obtain a clear image. This analysis showed the differences in morphological studies for CAC before and after adsorption with  $\text{Pb}(\text{NO}_3)_2$ .

### **Adsorption Parameters, Isotherm and Kinetics Studies**

#### ***Temperature of solution***

The initial concentration of  $\text{Pb}(\text{II})$  ions, pH, adsorbent dosage, and volume of  $\text{Pb}(\text{II})$  ions solution were all held constant to evaluate the effect of temperature. With a fixed volume of 100 mL, the initial concentration of  $\text{Pb}(\text{II})$  ions solution was 20 ppm. Approximately 0.5 g of CAC was used, and the pH level was fixed. An isothermal water bath shaker was used to keep the solution warm. The agitation speed has been set to 160 rpm. This batch's temperatures range from  $25^\circ\text{C}$ ,  $35^\circ\text{C}$ ,  $45^\circ\text{C}$ ,  $55^\circ\text{C}$ , and  $65^\circ\text{C}$ .

#### ***Initial concentration of the solution***

The solution temperature, adsorbent amount, and volume of  $\text{Pb}(\text{II})$  ion solution were all held constant in this study. 100 mL of  $\text{Pb}(\text{II})$  ions stock solution was used. Approximately 0.5g of CAC was used. The solution was kept at room temperature. The agitation speed has been set to 160 rpm. The initial concentration values used range from 1 ppm to 20 ppm.

#### ***Dosage of adsorbent***

The weight of the adsorbent used determined the adsorbent dosage. The initial concentration of  $\text{Pb}(\text{II})$  ions, solution temperature, solution pH, and volume of  $\text{Pb}(\text{II})$  ions solution were all held constant for this study. The volume used was 100 mL, and the pH was fixed. The  $\text{Pb}(\text{II})$  ions have an initial concentration of 20 ppm. The solution was kept at room temperature. The agitation speed has been set to 160 rpm. The adsorbent weights ranged from 0.5 g to 1.0 g, 1.5 g to 2.0 g, and 2.5 g.

To determine the kinetics and dynamic of the adsorption of  $\text{Pb}(\text{II})$  ions on the CAC, pseudo-first-order and pseudo-second-order were used. All kinetic tests were performed at room temperature without any variations in pH level. Data fitting was plotted in linear graph forms, and a suitable kinetics model was identified. Langmuir and Freundlich isotherm models were applied to fit the experimental equilibrium isotherm data to determine prepared CAC's maximum  $\text{Pb}(\text{II})$  ions adsorption capacity. All isotherms tests were performed at room temperature and constant pH. Data fitting was plotted in linear graph forms, and a suitable kinetics model was identified.

---

## RESULTS AND DISCUSSION

### Physical Characterization of CAC

Table 1 shows the physical characterization of CAC. The percentage yield of CAC activated with KOH in a 1:4 ratio was 67.3%, as shown in Table 1. The percentage of yield without KOH was 34.2%. According to Hui and Zaini (2015), the percentages yields of various types of AC made from organic waste activated using KOH are between 10 and 40%.

Increasing the activation ratios of KOH might enhance the yield by up to 80%. This study showed that the yield percentage improved from 34.2 to 67.3 %. CAC with KOH activation has a greater percentage yield than CAC without KOH activation. It proves that the percentage of yield grows when chemical activation happens.

**Table 1.** Physical characteristics of CAC activated with KOH

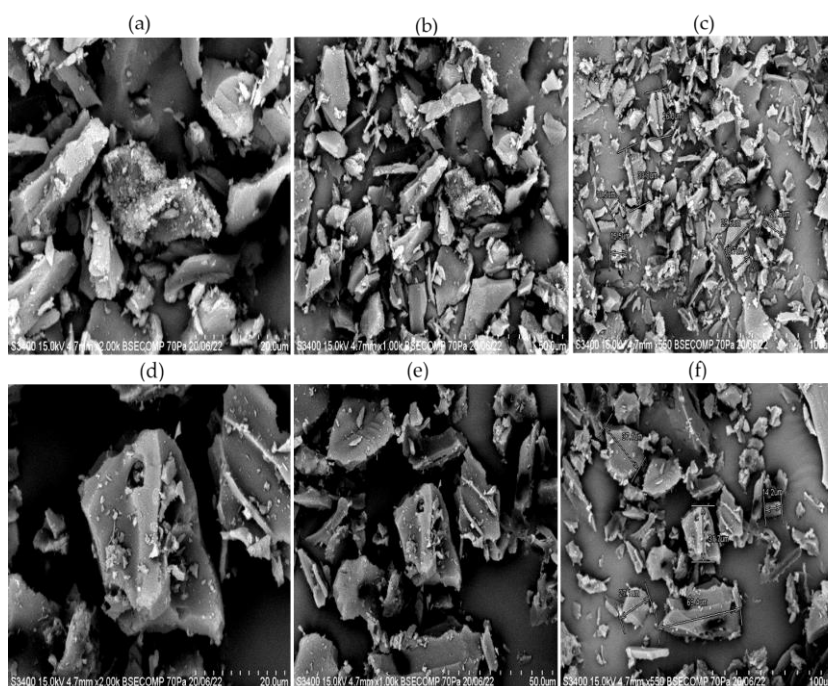
Parameter	Value
Percentage of yield, %	67.3
Bulk density, g/mL	0.44
Moisture content, %	3.25
pH	8.17

Table 1 shows that the bulk density of synthesized CAC is 0.44 g/mL. According to Buah and Kuma (2012), the bulk density of organic-based AC generated under varied parameters such as activation time, temperatures, and chemical activation was 0.40-0.57 g/mL. The moisture content of the CAC was 3.25% (Table 1). The moisture content for CAC is almost closer to the average moisture content level for various CAC. There was no discernible difference in the dosage of the chemical activation agent used. Although most of the moisture must be eliminated during the carbonization

procedure at high temperatures, the moisture content in such specimens could be attributable to the moisture absorption from the external environment post-activation. Although they may absorb moisture from their surroundings, they seem dry. Decreasing the moisture content improves AC effectiveness since vapors interact in the adsorption mechanism and occupy the sorption capacity inside the pore, limiting AC effectiveness. Moisture content has a massive effect on sorption efficiency. As it has been revealed that moisture retained mostly in CAC will interact with volatile organic compounds (VOCs), causing the prevalence of oxygen-containing organic compounds upon that CAC exterior, resulting in a reduction in adsorption efficiency and eventually slow adsorption exchange again for focused adsorbate.

The addition of chemical activation agents included in the source during the preparation method largely affects the pH value of CAC. The pH value achieved in this investigation was 8.17. It suggests that additional channels, including such contacts, hydrogen bonds, and hydrophobic interactions, might be involved in adsorption.

Figure 1 (a, b, c) shows the SEM images of CAC before adsorption, whereas Figure 1 (d, e, f) shows the SEM images of CAC after adsorption at different magnifications. The CAC's scattered, rough, and irregular shapes were observed in Figure 1(a, b, c). SEM was used to analyze the morphology of the CAC and estimate the average diameter of the CAC. The physical structural differences and the CAC's diameter increase are visible in Figures 1 (a-f). The SEM images were taken at an accelerating voltage of 15kV.



**Fig. 1:** SEM images of CAC before adsorption at magnification (a) 20  $\mu\text{m}$  (b) 50  $\mu\text{m}$  (c) 100  $\mu\text{m}$ , and after adsorption at magnification (d) 20  $\mu\text{m}$  (e) 50  $\mu\text{m}$  (f) 100  $\mu\text{m}$

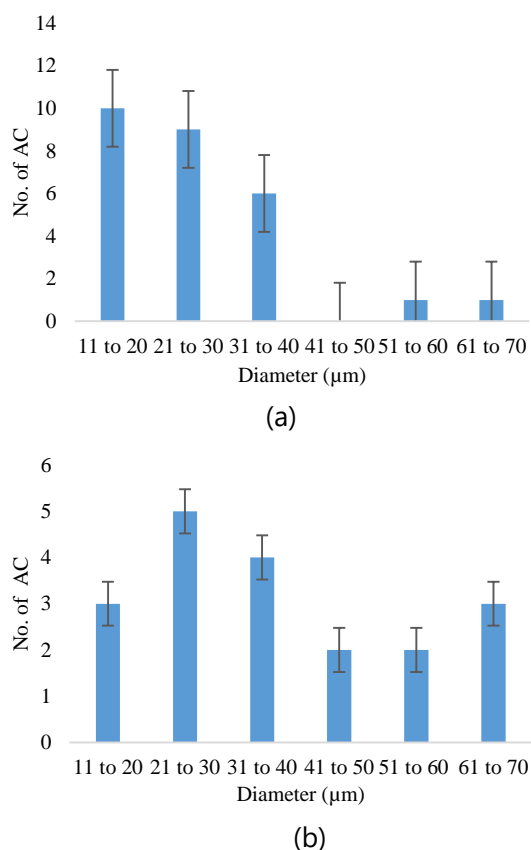
Figure 2(a) shows the number of fibers against the diameter before adsorption. Based on Figure 2(a), the average diameter of the CAC before adsorption is 25.11  $\mu\text{m}$ . The average diameter of the CAC was manually calculated by the overall diameter measurement obtained during the SEM analysis conducted for the CAC.

Figure 2(b) shows the number of fibers against the diameter after adsorption. Based on Figure 2(b), the average diameter of the CAC after adsorption is 39.21  $\mu\text{m}$ . The average diameter after adsorption is higher by comparing both plots in Figures 2(a) and 2(b). The increased thickness of the carrageenan proves the adsorption of lead ion occurs. Previous researchers stated that CAC adsorbs adsorbate and thickens after SEM analysis (Maharani et al., 2019; Mahdavinia et al., 2015). The deposition of Pb(II) ions onto the carrageenan surface due to the mixing of the CAC into the lead solution leads to the increased size of CAC

(Mahdavinia et al. 2015).

FTIR was utilized to identify CAC's chemical structure and functional groups by measuring infrared radiation absorption at various wavelengths. Figure 3(a) shows the FTIR of CAC before adsorption, whereas Figure 3(b) shows the FTIR of CAC after adsorption. The spectrum reveals the presence of common bands of functional groups such as hydroxyl, aldehyde, nitrile stretch, alkene, and carbonyls in carrageenan materials. The broad peak at 3300  $\text{cm}^{-1}$  to 3500  $\text{cm}^{-1}$  is referred to amine stretching vibration of the carrageenan properties. Whereas the bands at 1700  $\text{cm}^{-1}$  correspond to scissor vibrations of carbonyl stretching. Furthermore, the nitrile stretches linkages in CAC that correlate to the peak at 2260  $\text{cm}^{-1}$  to 2220  $\text{cm}^{-1}$  are frequently expressed. Glycosidic linkage vibrations were identified as a succession of peaks ranging from 1010  $\text{cm}^{-1}$  to 1080  $\text{cm}^{-1}$ . C-O-C stretching in 3,

6-anhydrogalactose are within the range of 980-940  $\text{cm}^{-1}$ , while nitrate ion vibration would be detected from 630  $\text{cm}^{-1}$  to 715  $\text{cm}^{-1}$  (Mandal et al., 2021; Kushwaha et al., 2017). The spectra of CAC after adsorption presents the bands of CAC, where new sharp peaks at 635  $\text{cm}^{-1}$  corresponded to the strong  $\text{NO}_3^-$  stretch vibration of the carbonyl ester of the CAC. This indicates that the adsorbate ( $\text{Pb}(\text{NO}_3)_2$ ) has been adsorbed into CAC and shows nitrate ion vibration in FTIR analysis. The intensity of these characteristic bands was significantly higher with increasing  $\text{Pb}(\text{NO}_3)_2$  ratio in the blends (Imamoglu et al., 2018). This is proved that  $\text{Pb}(\text{NO}_3)_2$  has been adsorbed onto CAC during the mixing process.



**Fig. 2;** Number of fibers against the diameter (a) before adsorption and (b) after adsorption

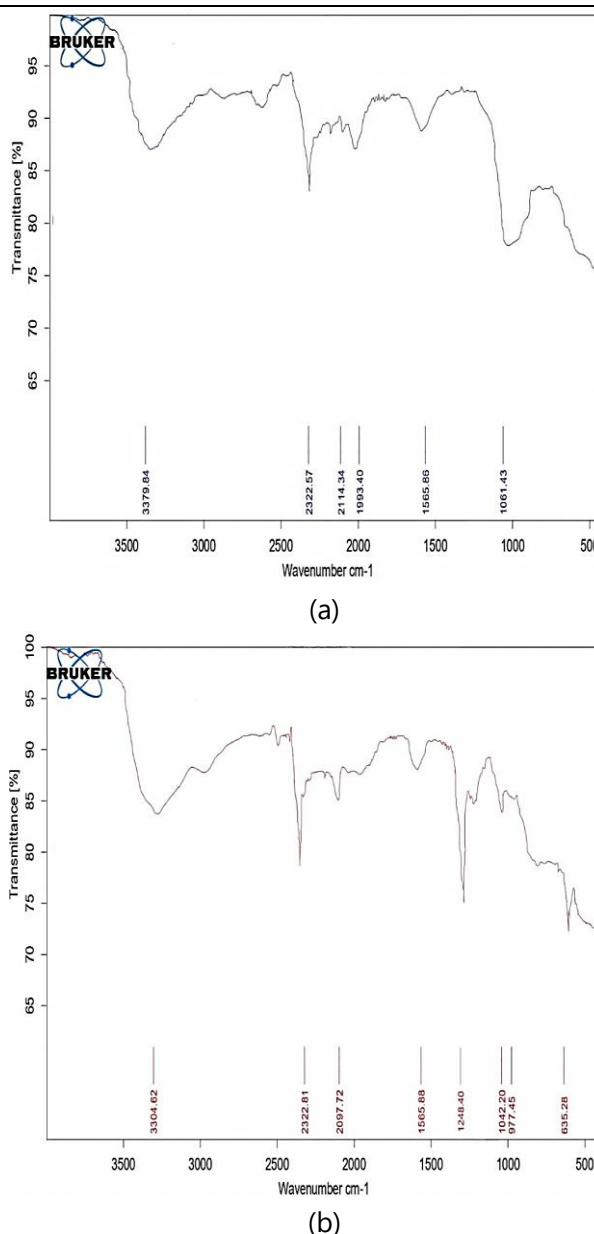


**Fig. 3:** FTIR of CAC (a) before and (b) after adsorption

Table 2 summarizes the predicted IR spectra and respective wavelengths of various functional groups present before and after the adsorption of  $\text{Pb}(\text{NO}_3)_2$  solution on CAC.

### Effects of Different Parameters

The adsorption results using various adsorbent dosages are presented in Table 3.

**Table 2.** Predicted peak identification of FTIR spectra of CAC before and after Pb(NO<sub>3</sub>)<sub>2</sub> adsorption

Wavelength, cm <sup>-1</sup>		Functional groups
Before adsorption	After adsorption	
3379.84	3304.62	Amine
2322.57	2322.81	Nitrile
1565.86	1565.88	Alkene
1061.43	1040.20	Glycosidic Linkage
-	977.45	C-O-C stretching in 3, 6-anhydrogalactose
-	635.28	NO <sub>3</sub> <sup>-</sup>

According to Çermikli et al. (2020), when the amount of adsorbent increases, the adsorption increases due to the large number of active sites of the AC. It enables a large number of lead ions to be adsorbed. However, Table 3 indicates that the adsorption is fast at the initial phase but slower at the final phase upon reaching equilibrium. According to a few researchers, this scenario happens due to the conglomeration of the active sites at dosages beyond the optimum (Çermikli et al., 2020; Momčilović et al., 2011; Santhy and Selvapathy, 2006). Based on Table 3, the removal amount of Pb(II) ions by CAC was observed to increase with an increase in the weight of AC. It also shows that the removal amount of 0.5 g of CAC was the lowest, and 2.5 g of CAC has the highest. This is because the availability of an active site for adsorption to lead ion for a higher dosage of CAC is plenty compared to the lower dosage of CAC. Thus, the adsorption capacity would be higher for higher dosages of CAC. This observation was attributed to the increased active adsorption sites available until

equilibrium was achieved. Lead removal by coconut pith AC and heartwood of areca catechu powder all exhibited comparable trends (Haloi et al. 2013, Santhy and Selvapathy 2006).

The experiment was set up with a constant weight of AC, 0.5 g with 0.1 l adsorbate, and a constant initial concentration of 20 ppm to study the effects of the temperature of Pb(II) ions solution on adsorption. The adsorption was conducted on the hot plate magnetic stirrer at different temperatures from 25°C to 65°C with 10°C intervals. The set-up experimental time was 1 h. Table 4 shows the Pb(II) ions adsorbed in 1 h using CAC at various Pb(II) ions solution temperatures.

Based on Table 4, when the temperature increases, the efficiency of Pb(II) ions adsorption increases until a certain point which is 45°C. This scenario has been reported in many studies as well. Due to an increase in temperature, the efficiency of the chemical groups in the lead ion increases, and the thermal energy of the adsorbate increases (Imamoglu et al., 2018). Hence, the strength of attractive forces between the lead ion and adsorbent increases. For example, by comparing the adsorption percentage after 1 hour at 25°C is 35.61%, whereas, at 45°C is 46.40%. Removal percentage is at optimum in 45°C based on the data obtained. As shown in Table 4, the Pb(II) ion's removal trend initially increased until a saturated point and started to drop back the removal percentage. The cause might be an increase in the rate of interparticle dispersion in the pore at higher temperatures. However, once the temperature was elevated to 45°C, the efficient removal rate for Pb(II) ions started dropping. The slight drop in removal percentage for Pb(II) ions at higher temperatures might be attributed to fewer

interactions between the adsorbent and the adsorbate. At higher temperatures, the active sites of CAC started to denature due to extreme heat and lowered the effectiveness of  $\text{Pb}(\text{NO}_3)_2$  adsorption onto CAC (Mandal et al., 2021).

The experiment was set up with a constant weight of AC, 0.5 g with 0.1

adsorbate, and various initial concentrations of Pb(II) ions solution to study the effects of the initial Pb(II) ions solution on adsorption. The adsorption was conducted on the hot plate magnetic stirrer at room temperature. The adsorption results using various initial concentrations are presented in Table 5.

**Table 3.** Amount of Pb(II) ions adsorbed for 1 hour using CAC at various dosages of adsorbent

Weight of AC, g	Volume of Pb(II), l	Initial concentration of Pb(II), ppm	Time, h	Concentration at time, $C_e$ , ppm	Adsorption capacity, $Q_e$ , mg/g	Removal percentage, %
0.5	0.1	20	1	12.75439	1.45	36.23
1	0.1	20	1	8.035088	1.20	59.82
1.5	0.1	20	1	0.684211	1.29	96.58
2	0.1	20	1	0.403509	0.98	97.98
2.5	0.1	20	1	0.192982	0.79	99.04

**Table 4.** Amount of Pb(II) ions adsorbed in 1 h using CAC at various temperatures of Pb(II) ions solution

Temperature, °C	Weight of CAC, g	Volume of Pb(II), l	Initial concentration of Pb(II), ppm	Time, h	Concentration at time, $C_e$ , ppm	Adsorption capacity, $Q_e$ , mg/g	Removal percentage, %
25	0.5	0.1	20	1	12.88	1.42	35.61
35	0.5	0.1	20	1	11.65	1.67	41.75
45	0.5	0.1	20	1	10.72	1.86	46.40
55	0.5	0.1	20	1	11.75	1.65	41.23
65	0.5	0.1	20	1	12.16	1.57	39.21

**Table 5.** Amount of Pb(II) ions solution adsorbed for 1 h using CAC at various initial concentrations

Weight of CAC (g)	Volume of Pb(II), l	Initial Concentration of Pb(II), mg/L	Time, h	Concentration at time, $C_e$ , mg/L	Adsorption capacity, $Q_e$ , mg/g	Removal percentage, %
0.5	0.1	1	1	0.053	0.19	94.74
0.5	0.1	5	1	0.316	0.94	93.68
0.5	0.1	10	1	1.263	1.75	87.37
0.5	0.1	15	1	5.246	1.95	65.03
0.5	0.1	20	1	12.754	1.45	36.23

Table 5 shows that an increase in initial concentration increases the amount of adsorbed Pb(II) ions. However, the removal percentage of Pb(II) ions differs. The result also shows that the adsorption capacity increases rapidly at the initial stages of contact time, whereas it slows down upon reaching its equilibrium point. Table 5 depicts the influence of initial Pb(II) ions concentrations ranging from 1 to 20 mg/L upon adsorption. The quantity of adsorbate was lower with lower starting adsorbate concentrations than higher concentrations. The removal of Pb(II) ions was shown to be dependent on the concentration, as decreasing the initial concentration enhanced the quantity of lead eliminated. While the percentage of lead removal was determined to be 94.74% at starting concentrations of 1 mg/, it was 36.23 % for concentrations of 20 mg/L.

The drastic rise in adsorption at the initial phase is due to the higher affinity of the interacting group on the surface of CAC, which slows down when the surface area of free activated sites of the CAC decreases (Santhy and Selvapathy, 2006). The relationship between Pb(II) ions and the CAC was also improved when the adsorbate concentration increased. The absorption capacity of the  $\text{Pb}(\text{NO}_3)_2$  was improved by increasing the starting concentration of Pb(II) ions from 1 ppm to 20 ppm, as shown in Table 5. Because of the abundant empty sites and functional groups on CAC, the rate of adsorption of Pb(II) ions was quick at first at all concentrations. When the concentration of the adsorbate was raised, there were two possible causes for the rise in adsorption capacity (i) more adsorbate molecules for adsorption onto CAC (ii) increased mass transfer, the driving force, which strengthened interactions in metal ions (Halo

et al., 2013). The obtained result revealed that the CAC has a good adsorption capacity and adsorption efficiency towards Pb(II) ions since the overall removal percentage after 1 h is more than 50% in four out of five initial concentrations.

### Adsorption Isotherm Analysis

The adsorption isotherm is calculated using equilibrium values. Its main purpose is to show how the adsorption molecule disperses between the liquid and solid phases when it reaches the symmetrical phase. A linear graph was plotted for Langmuir and Freundlich. Adsorption data analysis is necessary for constructing an equation that accurately captures the results and may be used for design considerations (Padmavathy et al., 2019). At constant temperature, the sorption isotherms express the precise relationship between sorbate concentration and degree of deposition on the sorbent surface. The nature and kind of the system influence the choice of an isotherm equation. The Langmuir model was considered by assuming that maximum adsorption occurs when a saturated monolayer of Pb(II) ions solution is present on the CAC. The adsorption energy is constant, and no adsorbate molecules are migrated in the surface plane (Kushwaha et al., 2017). Figure 4 shows the fittings of the Langmuir and Freundlich adsorption isotherm model.

Adsorption isotherms are determined under equilibrium or stable conditions. It shows how the adsorption particle distributes between the liquid and solid phases when it reaches equilibrium. The analysis was done to determine the most suitable isotherm model for the CAC. The applicability of the isotherm equation to define the adsorption process was determined by the correlation value,  $R^2$  values. Table 6 compares Langmuir and

Freundlich isotherms for the adsorption of Pb(II) ions by CAC.

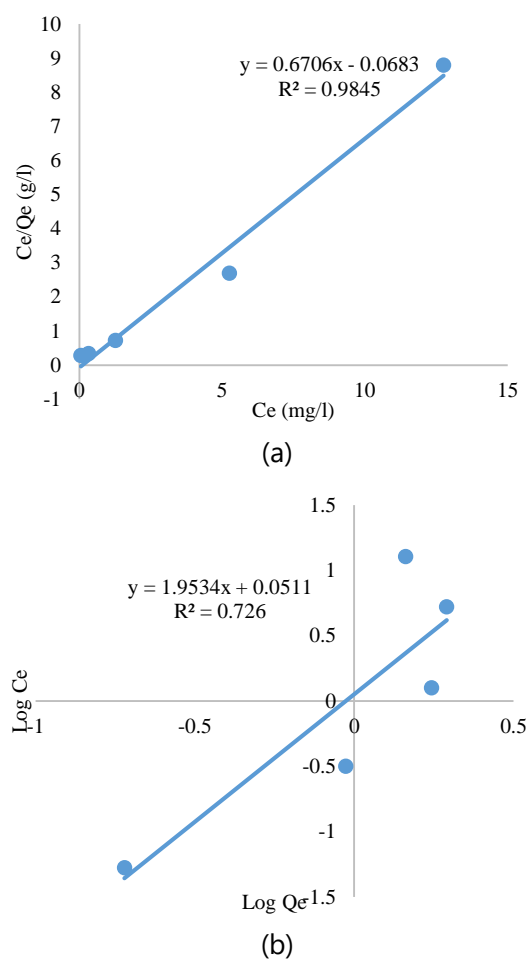


**Fig. 4:** Adsorption isotherm model for adsorption of Pb(II) ions by CAC (a) Langmuir adsorption isotherm (b) Freundlich adsorption isotherm

Based on Table 6, the  $R^2$  value obtained is 0.9845 for Langmuir and 0.7260 for Freundlich isotherm. Both isotherm models favor adsorbing Pb(II) ions by CAC. However, comparatively, the Langmuir model has higher reliability than Freundlich Model. The Langmuir model,  $Q_{max}$  which measures the monolayer adsorption capacity of the CAC, was calculated at 1.4912 mg/g for Pb(II) ions solution. The value of  $b$  was in the range from 0-10, indicating that the CAC adsorbent was suitable for Langmuir adsorption for Pb(II)

ions solution. For the Freundlich model, the value of  $n$  indicates the favorability and degree of heterogeneity. Adsorption is shown to be effective when  $n$  is around 1 and 10, adverse when  $n > 10$ , and irreversible if  $n < 1$ . Thus, this indicates that the Freundlich model could be more favorable than the Langmuir model. The Langmuir adsorption isotherm  $Q_{max}$  was used to compute theoretical maximum concentrations of adsorbate, and the results were quite similar to the experimentally observed values. The possible adsorption pathways of Pb(II) ions onto CAC may include pore diffusion through CAC's mesopores, surface complexation and electrostatic interactions between the surface functional (negative) groups of CAC and Pb(II) ions, precipitation, etc. (Girish and Murty, 2015).

**Table 6.** Data of comparison of adsorption isotherm model

	$1/Q_{max}$ , g/mg	0.6706
	$Q_{max}$ , mg/g	1.4912
Langmuir Isotherm	Intercept ( $1/Q_{max}b$ )	0.0683
	$b$ , l/mg	9.8184
	$R^2$	0.9845
	$R_L$	0.0011
	$1/n$	1.9534
	$n$	0.5119
Freundlich Isotherm	$\text{Log } K_F$	0.0511
	$K_F$	1.1248
	$R^2$	0.7260

### Adsorption Kinetic Model Analysis

Adsorption kinetics research is essential for determining the process and effectiveness of an adsorption process. Pb(II) ions kinetics in prepared AC was studied utilizing pseudo-first-order and pseudo-second-order kinetic

models. Figure 5 shows pseudo-first-order model and pseudo-second-order kinetics for the adsorption of Pb(II) ions by CAC.

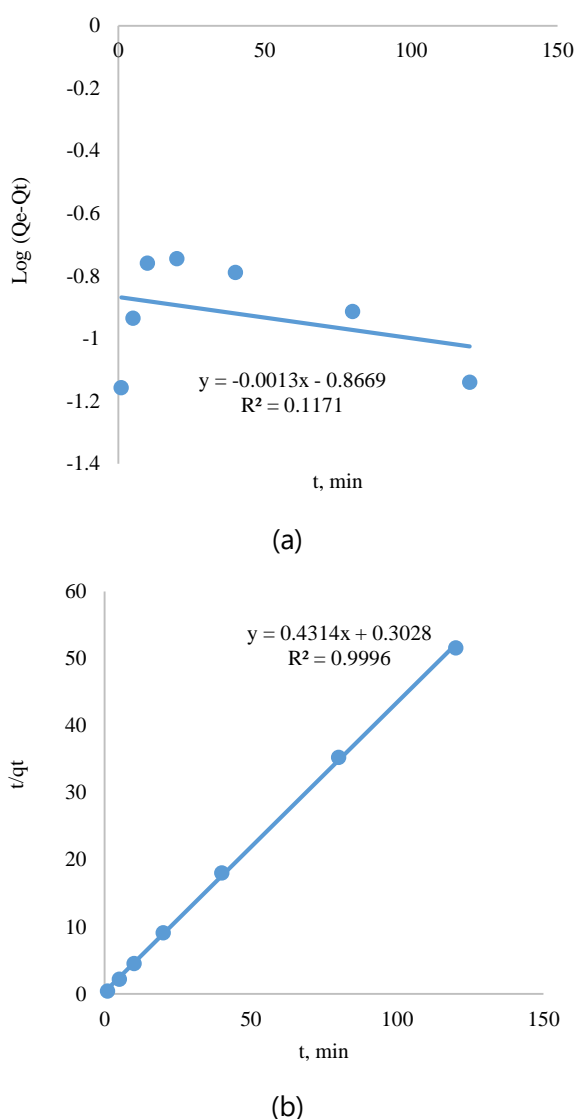


**Fig. 5:** Kinetics for adsorption of Pb(II) ions by CAC (a) Pseudo-first-order model (b) Pseudo-second-order model

Figure 5 shows that the Pb(II) ions adsorption rate was higher in the beginning (within an hour), indicating that the CAC adsorbent had more accessible active sites, culminating in a lot of Pb(II) ions adsorbed from aqueous solution. Furthermore, it demonstrates that, while Pb(II) ions adsorption was originally quite fast, it slowed with time and reached a constant value (equilibrium time). The initial quicker rate might be due to the adsorbents' exposed surface area being available.

Adsorption kinetics describes the rate of adsorbate uptake on the adsorbent, which controls the equilibrium time. The prediction of the adsorption rate is determined using the kinetics parameters for designing and modelling the processes. It functions similarly to adsorption isotherms, where the process is determined under equilibrium or stable conditions. The determined the most suitable kinetic models for the CAC. The applicability of the kinetic model equation to define the adsorption processes was determined by the correlation coefficient value,  $R^2$  values (Roy et al., 2022; Jahan et al., 2022). Table 7 shows the comparison of the adsorption kinetics of CAC.

The adsorption of CAC was best matched to a PSO kinetic model, as evidenced by the significant  $R^2$  of 0.9996, compared to a PFO kinetic model ( $R^2 = 0.1171$ ). The discovery of pseudo-second-order kinetics implies as Pb(II) ions sorption by CAC is an adsorptive mechanism. The equilibrium adsorption the entire variety of contact periods. That's

**Table 7.** The Comparison of adsorption kinetics of CAC

$Q_e$ (exp), mg/g	PFO			PSO		
	$Q_e$ (calc), mg/g	$K_1$ , h <sup>-1</sup>	$R^2$	$Q_e$ (calc), mg/g	$K_2$ , g/mg.h	$R^2$
2.56	0.997011	1.9965	0.1171	2.3180	0.1861	0.9996

capacities,  $Q_e$ , is required, and the second-order accuracy of proposed well over because the chemisorption mechanism is slower, causing adsorption quantity to stay much lower than the equilibrium state. As a result, the pseudo-first-order model did not accurately capture the adsorption kinetics in this investigation since  $Q_e$  is often achieved by experimentation. In all cases, including varying mixing times, as shown in Table 7, the projected values correspond well with the measured data in the Pseudo-second-order model with minimal fitting errors. Furthermore, the pseudo-second-order model's calculated  $Q_e$  ( $Q_{e \text{ (calc)}}$ ) was far more similar to the experimental  $Q_e$  ( $Q_{e \text{ (exp)}}$ ) than the pseudo first-order model's predicted values.

Therefore, the adsorption of Pb(II) ions onto CAC adsorbent could be a pseudo-second-order process rather than pseudo-first-order. For adsorbents such as agro-waste derived AC, the rate of adsorption reduced as the original heavy metal concentration increased (Gerçel and Gerçel, 2007; Rahman et al. 2014). The kinetic investigation revealed that a pseudo-second-order model best explained the adsorption of textile colors (acidic) on activated coconut shell carbon (Rahman et al., 2014). In addition, the adsorption of lead on the surface of CAC followed the pseudo-second-order model with a higher value of regression coefficient (0.989) obtained for the pseudo-second-order model compared with other models. Based on Mahdavinia et al. (2015), comparative kinetic studies have been conducted for the removal of organic compounds as well as heavy metals using kappa CAC, results are proven that pseudo-second-order kinetic models most favorable with greater regression coefficient,  $R^2$ .

## CONCLUSIONS

According to the findings, CAC can be synthesized from the hydrothermal method followed by chemical activation and carbonization. This study indicates that the average diameter of CAC is higher after adsorption (39.21  $\mu\text{m}$ ) than before adsorption (25.11  $\mu\text{m}$ ) in the SEM test. Its shows that Pb(II) ions have adsorbed onto the CAC and got thicker. The optimized operating variables were initial Pb(II) ions concentration of 1 ppm, a different temperature of 45°C and an adsorbent dosage of 2.5 g, which would result in the maximum removal percentage of Pb(II) ions in this study conducted. Throughout this study, the highest capacity of CAC was determined to be 1.95 mg/g, while the minimum capacity was found to be 0.19 mg/g. The Langmuir isotherm best represents the equilibrium data of CAC, with a maximum adsorption capacity of 1.95 mg/g. Langmuir isotherms model shows  $R^2$  value of 0.9845 compared to Freundlich isotherm model  $R^2$  value of 0.7260. Pseudo-second-order exhibited the best-fit data for kinetic studies with a regression coefficient of  $R^2$  0.9996, indicating that the adsorption of lead using CAC is limited by the chemisorption process.

## ACKNOWLEDGEMENTS

The authors sincerely thank Universiti Malaysia Sabah (UMS) for providing necessary research facilities to accomplish this study.

## REFERENCES

- Agasti, N., 2021. "Decontamination of heavy metal ions from water by composites prepared from waste." *Curr. Res. Green Sustain. Chem.*, 4, 100088.

- Alslaibi, T. M., Abustan, I., Ahmad M. A. and Foul, A. A., 2013. "A review: production of activated carbon from agricultural byproducts via conventional and microwave heating." *J. Chem. Technol. Biotechnol.*, 88, 1183-1190.
- Buah, W. and Kuma, J., 2012. "Properties of activated carbon prepared from coconut shells in Ghana." *Ghana Min. J.*, 13, 51-55.
- Çermikli, E., Şen, F., Altıok, E., Wolska, J., Cyganowski, P., Kabay, N., Bryjak, M., Arda, M. and Yüksel, M., 2020. "Performances of novel chelating ion exchange resins for boron and arsenic removal from saline geothermal water using adsorption-membrane filtration hybrid process." *Desalination*, 491, 114504.
- Gerçel, Ö. and Gerçel, H. F., 2007. "Adsorption of lead (II) ions from aqueous solutions by activated carbon prepared from biomass plant material of *Euphorbia rigida*." *Chem. Eng. J.*, 132(1-3), 289-297.
- Girish, C. and Murty, V. R., 2015. "Adsorption of phenol from aqueous solution using *Lantana camara*, forest waste: packed bed studies and prediction of breakthrough curves." *Environ. Process.*, 2(4), 773-796.
- Hassim, N. A. A., Hui, K. C., Floresyona, D., Kamal, N. A. and Sambudi, N. S., 2022. "Effect of pH on adsorption of  $\text{Cu}^{2+}$  by using composite of polyvinyl alcohol (PVA)/Kaolin." *ASEAN Journal of Chemical Engineering*, 22(1), 93-104.
- Haloi, N., Sarma, H. P., and Chakravarty, P., 2013. "Biosorption of lead (II) from water using heartwood charcoal of *Areca catechu*: equilibrium and kinetics studies." *Appl. Water Sci.*, 3(3), 559-565.
- Hui, T. S. and Zaini, M. A. A., 2015. "Potassium hydroxide activation of activated carbon: a commentary." *Carbon Lett.*, 16(4), 275-280.
- Imamoglu, M., Ozturk, A., Aydın S., Manzak, A., Gündoğdu, A. and Duran, C., 2018. "Adsorption of Cu (II) ions from aqueous solution by hazelnut husk activated carbon prepared with potassium acetate." *J. Dispers. Sci. Technol.*, 39(8), 1144-1148.
- Islam, M. S., Kwak, J. H., Nzediegwu, C., Wang, S., Palansuriya, K., Kwon, E. E., Naeth, M. A., El-Din, M. G., Ok, Y. S. and Chang, S. X., 2021. "Biochar heavy metal removal in aqueous solution depends on feedstock type and pyrolysis purging gas." *Environ. Pollut.*, 281, 117094.
- Jahan, N., Roy, H., Reaz, A. H., Arshi, S., Rahman, E., Firoz, S. H. and Islam, M. S., 2022. "A comparative study on sorption behavior of graphene oxide and reduced graphene oxide towards methylene blue." *Case Stud. Chem. Environ. Eng.*, 6, 100239.
- Jaishankar M., Tseten T., Anbalagan N., Mathew B. B. and Beeregowda K. N., 2014. "Toxicity, mechanism and health effects of some heavy metals." *Interdiscip. Toxicol.* 7(2), 60-72.
- Kamal K. H., Dacrory S., Ali S. S. M, Ali K. A. and Kamel S., 2019. "Adsorption of Fe ions by modified carrageenan beads with tricarboxy cellulose: kinetics study and four isotherm models." *Desalin. Water Treat.*, 165, 281-289.
- Kavand, M., Eslami, P. and Razeh, L., 2020. "The adsorption of cadmium and lead ions from the synthesis wastewater with the activated carbon: Optimization of the single and binary systems." *J. Water Process Eng.*, 34, 101151.
- Keshk, A. A., Elsayed, N. H., Zareh, M. M., Alenazi, D. A. K., Said, S., Alatawi, A. O., Albalawi, R. K., Maher, M., Algabry, S. M. and Shoueir, K., 2023. "Kappa-

- carrageenan for benign preparation of CdSeNPs enhancing the electrochemical measurement of AC symmetric supercapacitor device based on neutral aqueous electrolyte." *Int. J. Biol. Macromol.*, 234, 123620.
- Khan A., Goepel, M., Colmenares, J. C. and Gläser, R., 2020. "Chitosan-based N-doped carbon materials for electrocatalytic and photocatalytic applications." *ACS Sustain. Chem. Eng.*, 8(12), 4708-4727.
- Kushwaha, A. K., Gupta, N. and Chattopadhyaya, M. C., 2017. "Adsorption behavior of lead onto a new class of functionalized silica gel." *Arab. J. Chem.*, 10(1), S81-S89.
- Kwak, J. H., Islam, M. S., Wang, S., Messele, S. A., Naeth, M. A., El-Din, M. G. and Chang, S. X., 2019. "Biochar properties and lead(II) adsorption capacity depend on feedstock type, pyrolysis temperature, and steam activation." *Chemosphere*, 231, 393-404.
- Laksono H, Dyah C. K., Putri R. P. G., Soraya M., Purwoto H., 2022. "Characteristics of rapid visco analyzer carrageenan extract with enzymatic pretreatment of *Kappaphycus striatum*." *ASEAN Journal of Chemical Engineering*, 22 (2), 326-336.
- Lapwanit, S., Sooksimuang, T. and Trakulsujaritchok, T., 2018. "Adsorptive removal of cationic methylene blue dye by kappa-carrageenan/poly (glycidyl methacrylate) hydrogel beads: preparation and characterization." *J. Environ. Chem. Eng.*, 6(5), 6221-6230.
- Lee J. W., Choi H., Hwang U. K., Kang J. C., Kang Y. J., Kim K. I. and Kim J. H., 2019. "Toxic effects of lead exposure on bioaccumulation, oxidative stress, neurotoxicity, and immune responses in fish: A review." *Environ. Toxicol. Pharmacol.*, 68, 101-108.
- Maharani, C. A., Budiasih, E. and Wonorahardjo, S., 2019. "Preparation and characterization of silica-carrageenan adsorbent for Pb<sup>2+</sup> and Cd<sup>2+</sup> as interfering ion." *IOP Conf. Ser.: Mater. Sci. Eng.* 546, 042021, 1-8
- Mahdavinia, G. R., Bazmizeynabad, F. and Seyyedi, B., 2015. "Kappa-Carrageenan beads as new adsorbent to remove crystal violet dye from water: adsorption kinetics and isotherm." *Desalin. Water Treat.*, 53(9), 2529-2539.
- Mandal S., Jose Calderon, J., Marpu S. B., Omary, M. A. and Shi S. Q., 2021. "Mesoporous activated carbon as a green adsorbent for the removal of heavy metals and Congo red: characterization, adsorption kinetics, and isotherm studies." *J. Contam. Hydrol.*, 243, 103869.
- Momčilović, M., Purenović, M., Bojić, A., Zarubica, A. and Randelović, M., 2011. "Removal of lead (II) ions from aqueous solutions by adsorption onto pine cone activated carbon." *Desalination*, 276(1-3), 53-59.
- Neme, I., Gonfa, G. and Masi, C., 2022. "Activated carbon from biomass precursors using phosphoric acid: A review." *Heliyon*, 8(12), e11940.
- Nogueira, J., António, M., Mikhalev, S. M., Fateixa, S., Trindade, T. and Daniel-Da-Silva, A. L., 2018. "Porous Carrageenan-derived carbons for efficient ciprofloxacin removal from water." *Nanomaterials*, 8(12) 1004.
- Padmavathy, K., Madhu, G. and Haseena, P. 2016., "A study on effects of pH, adsorbent dosage, time, initial concentration and adsorption isotherm study for the removal of hexavalent chromium (Cr (VI)) from wastewater by

- 
- magnetite nanoparticles." *Proc. Technol.*, 24, 585-594.
- Rahman, M. M., Adil, M., Yusof, A. M., Kamaruzzaman, Y. B. and Ansary, R. H., 2014. "Removal of heavy metal ions with acid activated carbons derived from oil palm and coconut shells." *Materials*, 7(5), 3634-3650.
- Roy, H., Islam M. S., Arifin, M. T. and Firoz, S. H., 2022. "Chitosan-ZnO decorated Moringa oleifera seed biochar for sequestration of methylene blue: Isotherms, kinetics, and response surface analysis." *Environ. Nanotechnol. Monit. Manag.*, 18, 100752.
- Santhy, K. and Selvapathy, P., 2006. "Removal of reactive dyes from wastewater by adsorption on coir pith activated carbon." *Bioresour. Technol.*, 97(11), 1329-1336.
- Song X., Liu H., Cheng, L. and Qu, Y., 2010. "Surface modification of coconut-based activated carbon by liquid-phase oxidation and its effects on lead ion adsorption." *Desalination*, 255(1-3), 78-83.
- Wang S., Kwak, J. H., Islam, M. S., Naeth, M. A., El-Din, M. G. and Chang, S. X., 2020. "Biochar surface complexation and Ni (II), Cu (II), and Cd (II) adsorption in aqueous solutions depend on feedstock type." *Sci. Total Environ.*, 712, 136538.
- Yahya, M. D., Obayomi, K. S., Abdulkadir, M. B., Iyaka, Y. A. and Olugbenga A. G., 2020. "Characterization of cobalt ferrite-supported activated carbon for removal of chromium and lead ions from tannery wastewater via adsorption equilibrium." *Water Sci. Eng.*, 13(3), 202-213.
-